Influence of shot peening on surface-layer characteristics of a monocrystalline nickel-based superalloy

Y. H. Chen
School of Materials Science and Engineering, Shanghai Jiao Tong University, Shanghai 200240, China and School of Physical Science and Technology, Xinjiang University, Urumqi 830046, China

C. H. Jiang,[a] Z. Wang, and K. Zhan
School of Materials Science and Engineering, Shanghai Jiao Tong University, Shanghai 200240, China

(Received 23 September 2010; accepted 26 September 2010)

Shot peening was conducted on [100]- and [111]-oriented monocrystalline nickel-based superalloy samples to study the effect of crystal orientation on the distributions of the residual stress and evolution of microstructures in the deformation layers on the sample surfaces as a function of the coverage up to 400%. The XRD results show that the orientation randomizations and the values of compressive residual stress in the [111]-oriented samples are relatively higher than those in the [001]-oriented samples. Moreover, the residual-stress distribution in each sample is anisotropic, and the residual stress is maximum along the ⟨110⟩ direction. This phenomenon can be explained by the anisotropic properties of a single-crystal alloy and mechanism of the dislocation slip in the plastic deformation layers. Line profile analysis was also used to obtain microstructural information of the samples. © *2010 International Centre for Diffraction Data.* [DOI: 10.1154/1.3506379]

Key words: shot peening, nickel alloy, residual stress, microstructure, line profile analysis, X-ray powder diffraction

I. INTRODUCTION

Monocrystalline nickel-based superalloys, having a face-centered-cubic (fcc) crystal structure, are widely used in aircraft, power-generation turbines, rocket engines, and other challenging environments, including nuclear power and chemical processing plants (Pollock and Tin, 2006; Leidermark *et al.*, 2009). These alloys have superior thermal, fatigue, and creep properties compared to conventional cast alloys because grain boundaries have been eliminated (Huang *et al.*, 2009; Prasad *et al.*, 2005). During the production route of turbine blades and services, the surface is treated mechanically, which resulted in a plastic deformation layer on the surface, and thus directly affects several important properties and characteristics of the machine (Pollock and Tin, 2006; Webster and Ezeilo, 2001).

In order to improve the performance of engineering components, shot peening (SP), a mechanical surface treatment, has been used widely (Boeckels and Wagner, 2005; Harada *et al.*, 2007). In this process, in-plane compressive residual stress (CRS) and work hardening are introduced into the surface layers of metallic components simultaneously by the impingement of a stream of shot directed at the metal surface at high velocity and controlled conditions (Tian *et al.*, 2008; Hammersley *et al.*, 2000; Kim *et al.*, 2005). These factors together with the refined grain size could distinctly affect the mechanical behavior of the material. It has been shown that, when properly controlled, SP can indeed enhance the tensile properties of the C-2000 nickel-based alloy (Kim *et al.*, 2005). However, up to now, studies of nickel-based alloys focus mainly on nanocrystallization (Villegas *et al.*, 2005; Villegas and Shaw, 2009) and rafting microstructure (Pollock and Tin, 2006; Touratier *et al.*, 2009) in the deformation layer induced by the shot peening process. Up to now the residual-stress distribution and the effect of crystallographic orientation on the surface-layer characteristics during SP have been rarely reported.

In this work, a SP process was applied to bulk samples of DD3, a nickel-based superalloy. The influence of crystallographic orientation on the residual-stress distribution of the residual stress and evolution of microstructure in the deformation layers after SP with various degrees of peening coverage have been investigated by X-ray diffraction (XRD). Line profile analysis (LPA) was also used to obtain microstructural information on the samples.

II. EXPERIMENTAL

The material examined in this paper is the monocrystalline Ni-based superalloy, DD3 (Ni, 9.5 Cr, 5.9 Al, 2.2 Ti, 5.2 W, 5 Co, 3.8 Mo, in wt %). The material was solution heat treated for 4 h at 1250 °C and subsequently air cooled to room temperature (RT), followed by a stage ageing process with 32 h at 870 °C. Two sets of samples were machined from cast bars: one with its longitudinal axis runs parallel to the [001] direction and the other parallel to the [111] direction. The deviation from the ideal orientation of each sample was less than 5°. Before SP, all samples were polished electrolytically. The gauge of each sample was shot peened at RT according to the conditions of 0.3 MPa jet pressure, 0.2 mm average diameter of ceramic beads, 100 mm distance between nozzle and specimen, and 0.6 mm N Almen peening intensity. The degrees of peening coverage, defined as ratio of the dimpled surface to the total surface after SP, for each set of the samples were 80%, 200%, and 400%.

The residual stresses were determined with Cr $K\alpha$ radiation using the (220) diffraction peak. The analysis was based on the $\sin^2\psi$ method. Young's modulus of $E=115$ GPa and

[a]Author to whom correspondence should be addressed. Electronic mail: chenyanhua97@163.com

Poisson's ratio of ν=0.3 were used to calculate the residual stresses from the observed lattice strains, without considering the elastic anisotropy. X-ray powder diffraction patterns were recorded using a Dmax/rc X-ray diffractometer with Cu $K\alpha$ radiation. Other experimental conditions are 40 kV, 100 mA, continuous scan, 30°–100° 2θ, and 0.02° 2θ step size. The domain size and microstrain in the deformation layer of each sample were estimated from the XRD pattern with the Voigt method (Langford, 1978). The relationship of integral breadths is given by

$$\beta_{fL} = \beta_{hL} - \beta_{gL}, \quad \beta_{fG}^2 = \beta_{hG}^2 - \beta_{gG}^2, \tag{1}$$

where subscript L and G denote the Lorentzian and Gaussian components and h, f, and g denote the measured line profile, the structurally broadened profile, and the instrumental profile, respectively. The as-received (or annealed) sample was used as the standard. For all profiles, the backgrounds were subtracted. Using Eq. (1), β_{fL} and the β_{fG} can be calculated, and then the microstructure was obtained. Using the Voigt method, with an assumption of the Lorentzian "size" and the Gaussian "microstrain" profiles for the domain size and microstrain, respectively, are given by

$$D = \lambda/\beta_{fL}\cos(\theta), \quad \varepsilon = \beta_{fG}/4\tan(\theta). \tag{2}$$

The broadening for low-angle reflections mainly relates to the domain size, and the broadening at high-angle reflections is predominantly determined by the internal strain (Villegas *et al.*, 2005; Shaw *et al.*, 2003). In this study, Ni (111) was used to calculate the domain size D, while Ni (311) was employed to estimate the microstrain ε. The dislocation density was calculated by the modified Warren-Averbach (MWA) method (Ungár and Borbély, 1996; Ungár *et al.*, 2001).

III. RESULTS AND DISCUSSION

A. Microstructure

Figure 1 shows the XRD patterns of the [001]- and [111]-oriented samples with the values of SP coverage of 80%, 200%, and 400%. Line broadening of the diffraction peaks was detected at all values of coverage (Figure 1), indicative of grain refinement and presence of lattice microstrain at and near the surface. Table I shows the values of grain size and microstrain estimated from Eq. (2) as well as the dislocation density calculated using the MWA method for these samples. Clearly, nanograins have formed at the surface region even at 80% coverage. With increasing peening coverage, a continuous broadening of the diffraction peaks and decreasing diffraction intensities were observed. These observations indicate an increase in the degree of lattice disorder and a decrease in the grain size. In other words, SP can randomize preexisting texture and the randomization effect increases with increasing coverage.

A decrease in domain size and increases in microstrain and dislocation density with increasing coverage are observed. It should also be noted that the domain size of each oriented samples was found to be about 30 nm, while the microstrains in the [111]-oriented samples are slightly larger than those in the [001]-oriented samples. This indicates that the crystallographic orientation of a sample has little effect on the domain-size distribution. Comparing the XRD patterns, the orientation randomizations in the [111]-oriented samples are much higher than those in the [001] oriented samples, especially the samples with 80% coverage. This implies that there is more extensive plastic deformation in the [111]-oriented samples. This difference comes from the fact that the elastic modulus in the ⟨111⟩ directions of Ni is considerably larger, and hence a smaller displacement is required in those directions to trigger plastic deformation (Huang *et al.*, 2009). Therefore, plastic deformation is more extensive in the ⟨111⟩ directions, which results in higher orientation randomization and lower texture intensity.

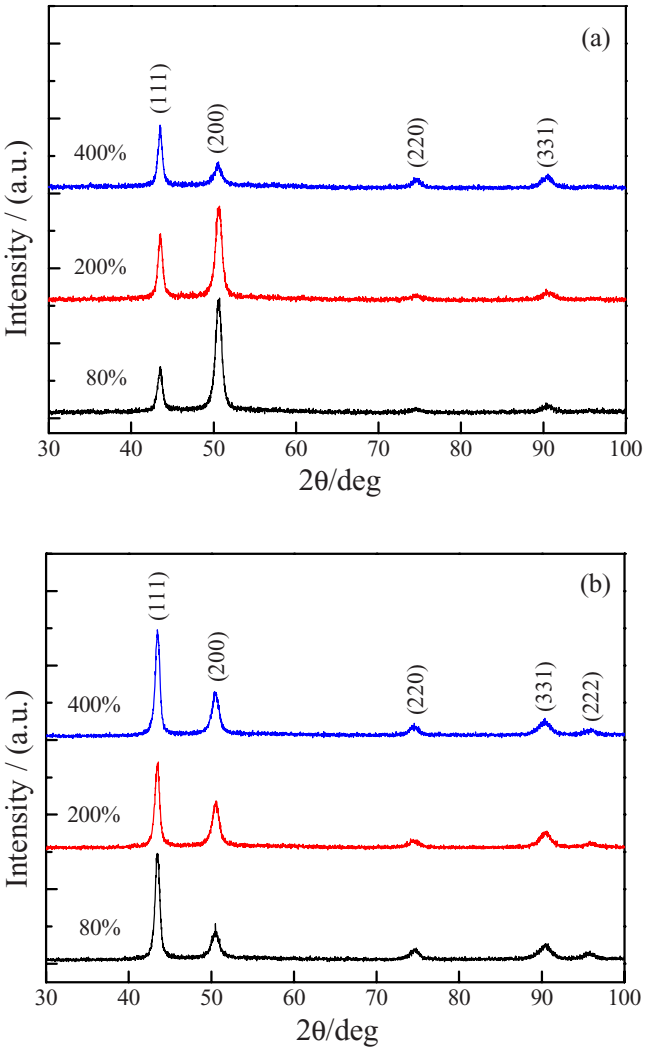

Figure 1. (Color online) Evolution of the XRD patterns for the DD3 alloy with coverage during SP: (a) [001]-oriented sample and (b) [111]-oriented sample.

B. Residual stress

Considering the anisotropic properties of the single-crystal alloys, the residual stresses at various φ angles were measured. The residual-stress distributions of the 80% and the 400% coverage samples are depicted in Figure 2. For both [001]- and [111]-oriented samples, the residual stresses at the surfaces are compressive. Moreover, the profiles and characters of CRS are similar. The value of CRS increases with increasing coverage. It is well known that the amount of

https://doi.org/10.1154/1.3506379 Published online by Cambridge University Press

TABLE I. Estimated domain size, microstrain, and dislocation density in SP-processed DD3 specimens from XRD experiments.

Sample	[001] orientation				[111] orientation			
Coverage/%	0	80	200	400	0	80	200	400
Domain size/nm	>1000	36	29	30	>1000	34	30	31
Microstrain	⋯	5.6×10^{-3}	5.9×10^{-3}	6.5×10^{-3}	⋯	6.2×10^{-3}	6.4×10^{-3}	7.1×10^{-3}
Dislocation density/m^{-2}		7.18×10^{15}	8.19×10^{15}	9.79×10^{15}		6.57×10^{15}	9.83×10^{15}	9.85×10^{15}

plastic deformation is responsible for the magnitude of surface residual stress (Harada and Mori, 2005). The degree of plastic deformation also increases with increasing coverage. Hence, the value of CRS is larger at a higher coverage. It should also be noted that the value of CRS in the [111]-oriented sample is relatively higher than that in the [001]-oriented sample at same coverage. Because during plastic deformation, the anisotropy in elastic modulus (Li *et al.*, 1994) leads to yield strength anisotropy along different crystallographic directions, the yield strength along the [111] direction is generally higher than that along the [001] direction. On the other hand, the mechanical properties of the shot-peened samples have an important influence in their CRS values, and there is a close linear relationship between surface residual stress (σ_{srs}) and the yield strength ($\sigma_{0.2}$).

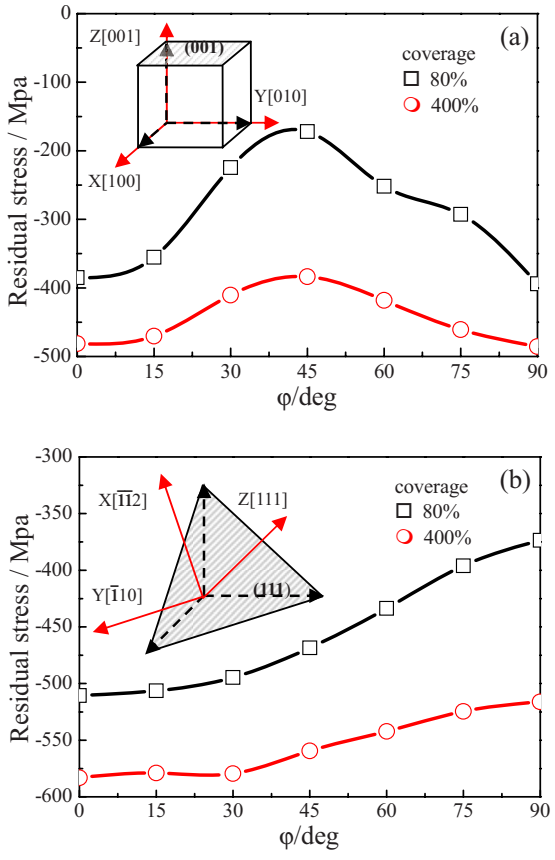

Figure 2. (Color online) Distributions of the residual stress of the DD3 alloy at 80% and 400% coverages. The illustration in top-left corner of the pattern shows the definition of corresponding sample orientation, where the *X* and *Y* axes correspond to $\varphi=0°$ and 90°, respectively: (a) [001]-oriented sample and (b) [111]-oriented sample.

Hence, the CRS value is larger in a sample with higher yield strength, processed under the same condition (Gao *et al.*, 2002; Wang *et al.*, 1998).

Moreover, for each sample, the distribution of the residual stresses is anisotropic and significantly lower along the ⟨110⟩ directions. In the [001]-oriented sample, the maximum CRS appears along the ⟨100⟩ directions ($\varphi=0°$ and 90°), where $\sigma_{srs}^{\langle 110\rangle}<\sigma_{srs}^{\langle 010\rangle}$. For the [111]-oriented sample, the CRS value was maximum along the ⟨112⟩ direction ($\varphi=0°$), where $\sigma_{srs}^{\langle 110\rangle}<\sigma_{srs}^{\langle 112\rangle}$. This is because the primary slip systems in a fcc material are the {111} planes in the ⟨110⟩ directions. During plastic deformation, dislocations slip along the ⟨110⟩ directions, which lead to a smaller CRS value. It is also been observed that, at a higher coverage, the anisotropic distribution of residual stress was weakened distinctly. This is attributed to larger plastic deformation, which can significantly induce grain-orientation randomization. Consequently, the influence of the preexisting texture on the distribution of residual stress diminishes. This result is consistent with the conclusion drawn from the XRD analysis discussed above.

IV. CONCLUSION

The microstructure and distribution of the residual stresses of DD3 nickel-based alloy subjected to a SP treatment have been investigated. The results show that crystallographic orientation plays an important role in the evolution of microstructure and the distribution of the residual stress. The following conclusion may be drawn:

(i) The SP processing can weaken the preexisting texture, and the randomization effect can be improved at a high coverage.

(ii) XRD analysis reveals that the orientation randomization in the [111]-oriented sample is relatively higher than that in the [001]-oriented sample, which is attributed to a higher elastic modulus and consequently extensive plastic deformation in the [111] direction.

(iii) LPA shows that the domain size appears to be ~30 nm, while the microstrain in the [111]-oriented sample is slightly larger, implying that the crystallographic orientation has little effect on the grain-size distribution.

(iv) Compared to the [001]-oriented sample, the value of CRS in the [111]-oriented sample is much larger, which can be explained by the linear relationship between σ_{srs} and $\sigma_{0.2}$, and $\sigma_{0.2}^{(111)}>\sigma_{0.2}^{(100)}$.

(v) The distribution of residual stresses is anisotropic, being significantly lower along the ⟨110⟩ directions,

https://doi.org/10.1154/1.3506379 Published online by Cambridge University Press

which is attributed to the ⟨110⟩ directions being the main slip directions in plastic deformation.

(vi) The anisotropic distribution of residual stress can be weakened distinctly at a high coverage. This is attributed to larger plastic deformation, which can significantly induce grain-orientation randomization.

ACKNOWLEDGMENT

Financial support from the National Natural Science Foundation of China under Project No. 50771066 is acknowledged.

Boeckels, H. and Wagner, L. (**2005**). "Effect of prior cold work on fatigue performance of shot peened Ti-2.5Cu," *Proceedings of the Ninth ICSP*, edited by V. Schulze and A. Niku-Lari (ICSP, Paris), pp. 332–337.

Gao, Y. K., Yao, M., and Li, J. K. (**2002**). "An analysis of residual stress fields caused by shot peening," Metall. Mater. Trans. A **33**, 1775–1778.

Hammersley, G., Hackel, L. A., and Harris, F. (**2000**). "Surface prestressing to improve fatigue strength of components by laser shot peening," Opt. Lasers Eng. **34**, 327–337.

Harada, Y., Fukaura, K., and Haga, S. (**2007**). "Influence of microshot peening on surface layer characteristics of structural steel," J. Mater. Process. Technol. **191**, 297–301.

Harada, Y. and Mori, K. (**2005**). "Effect of processing temperature on warm shot peening of spring steel," J. Mater. Process. Technol. **162–163**, 498–503.

Huang, X., Gibson, T. E., Zhang, M., and Neu, R. W. (**2009**). "Fretting on the cubic face of a single-crystal Ni-base superalloy at room temperature," Tribol. Int. **42**, 875–885.

Kim, S. B., Evans, A., Shackleton, J., Bruno, G., Preuss, M., and Withers, P. J. (**2005**). "Stress relaxation of shot-peened UDIMET 720Li under solely elevated-temperature exposure and under isothermal fatigue," Metall. Mater. Trans. A **36**, 3041–3053.

Langford, J. I. (**1978**). "A rapid method for analysing the breadths of diffraction and spectral lines using the Voigt function," J. Appl. Crystallogr. **11**, 10–14.

Leidermark, D., Moverare, J. J., Simonsson, K., Sjöström, S., and Johansson, S. (**2009**). "Room temperature yield behaviour of a single-crystal nickel-base superalloy with tension-compression asymmetry," Comput. Mater. Sci. **47**, 366–372.

Li, S. X., Ellison, E. G., and Smith, D. J. (**1994**). "The influence of orientation on the elastic and low cycle fatigue properties of several single crystal nickel base superalloys," J. Strain Anal. Eng. Des. **29**, 147–153.

Pollock, T. M. and Tin, S. (**2006**). "Nickel-based superalloys for advanced turbine engines: Chemistry, microstructure, and properties," J. Propul. Power **22**, 361–374.

Prasad, S. C., Rao, I. J., and Rajagopal, K. R. (**2005**). "A continuum model for the creep of single crystal nickel-base superalloys," Acta Mater. **53**, 669–679.

Shaw, L., Luo, H., Villegas, J., and Miracle, D. (**2003**). "Thermal stability of nanostructured $Al_{93}Fe_3Ti_2Cr_2$ alloys prepared via mechanical alloying," Acta Mater. **51**, 2647–2663.

Tian, J. W., Dai, K., Villegas, J. C., Shaw, L., Klarstrom, D. L., and Ortiz, A. L. (**2008**). "Tensile deformation behavior of a nickel alloy subjected to surface severe plastic deformation," Mater. Sci. Eng., A **493**, 176–183.

Touratier, F., Andrieu, E., Poquillon, D., and Viguier, B. (**2009**). "Rafting microstructure during creep of the MC2 nickel-based superalloy at very high temperature," Mater. Sci. Eng., A **510–511**, 244–249.

Ungár, T. and Borbély, A. (**1996**). "The effect of dislocation contrast on X-ray line broadening: A new approach to line profile analysis," Appl. Phys. Lett. **69**, 3173–3175.

Ungár, T., Gubicza, J., Ribárik, G., and Borbély, A. (**2001**). "Crystallite size-distribution and dislocation structure determined by diffraction profile analysis: Principles and practical application to cubic and hexagonal crystals," J. Appl. Crystallogr. **34**, 298–310.

Villegas, J. C., Dai, K., Shaw, L. L., and Liaw, P. K. (**2005**). "Nanocrystallization of a nickel alloy subjected to surface severe plastic deformation," Mater. Sci. Eng., A **410–411**, 257–260.

Villegas, J. C. and Shaw, L. L. (**2009**). "Nanocrystallization process and mechanism in a nickel alloy subjected to surface severe plastic deformation," Acta Mater. **57**, 5782–5795.

Wang, S., Li, Y., and Wang, R. (**1998**). "Compressive residual stress introduced by shot peening," J. Mater. Process. Technol. **73**, 64–73.

Webster, G. A. and Ezeilo, A. N. (**2001**). "Residual stress distributions and their influence on fatigue lifetimes," Int. J. Fatigue **23**, 375–383.